Available online at www.sciencedirect.com

ScienceDirect

IFAC Papers Online CONFERENCE PAPER ARCHIVE

IFAC-PapersOnLine 49-11 (2016) 722–729

Effects of Differential Pressure Measurement Characteristics on Low Pressure-EGR Estimation Error in SI-Engines ⋆

Rani Kiwan * **Anna G. Stefanopoulou** * **Jason Martz** *
Gopichandra Surnilla ** **Imtiaz Ali** ** **Daniel Joseph Styles** **

* *University of Michigan, Ann Arbor, MI 48109, USA (e-mail: rkiwan@umich.edu).*
** *Ford Motor Company, Dearborn, MI, USA*

Abstract: With proper control, cooled LP-EGR can be used for knock mitigation in SI engines, enabling fuel economy improvements through more optimal combustion phasing and lower fuel-enrichment at high loads. In addition, it can allow more aggressive downsizing and boosting. Due to the inherent pressure pulsations and low differential pressures across the EGR valve, however, estimating the LP-EGR within the inducted charge can be problematic. The accuracy of this estimation, based on a pressure differential (ΔP) measurement and the steady compressible flow orifice equation is investigated for various ΔP sensor response speeds and sampling rates using a GT-Power model of a modified Ford 1.6 L EcoBoost engine. In addition, an unsteady compressible flow orifice equation that accounts for flow inertia is derived and used to estimate LP-EGR for the case of a fast response ΔP sensor. Errors in the estimated EGR percentage using the steady compressible orifice equation with averaged ΔP measurement can be as high as 30%, and errors within $\pm 1\%$ require a ΔP of at least 10 kPa. These two measures can be improved up to a maximum EGR estimation error of 10% and a minimum ΔP of 4 kPa respectively through the use of crank-angle resolved ΔP measurement. Further improvements are possible with the new unsteady orifice equation, where all errors are reduced roughly to within $\pm 1\%$. The effect of inertia, however, can be mimicked in the steady orifice equation with a realistic sampling rate and a slower sensor with an appropriately selected response speed, resulting in a maximum error of 5% and errors within $\pm 1\%$ for ΔP exceeding 1 kPa.

Keywords: Low pressure exhaust gas recirculation, Differential pressure measurement, Error analysis, Estimation algorithms, Pulsating flow.

1. INTRODUCTION

Future spark ignited (SI) engine designs are moving towards further downsizing and boosting to comply with increasingly stringent fuel economy regulations. While the reduced displacement shifts the engine's operation under normal driving conditions to regions with lower pumping and reduced relative frictional losses, turbocharging must be used to maintain performance. Unfortunately, the extent to which an SI engine can be downsized and boosted is constrained in part by knock. Knock can be mitigated by retarding spark timing at the expense of efficiency. While the resulting excessive exhaust temperatures can be further mitigated by fuel enrichment, such strategies further penalize efficiency (Teodosio et al. (2015); Potteau et al. (2007); Alger et al. (2008)).

Though knock propensity is increased with the use of internal exhaust gas recirculation (EGR) (Westin et al. (2000)), cooled external EGR reduces both knock tendency and exhaust gas temperatures (Teodosio et al. (2015); Potteau et al. (2007); Alger et al. (2008); Hoepke et al. (2012)). Hence, the use of external EGR can potentially improve the engine efficiency at high loads by allowing more optimal combustion phasing and less fuel enrichment. Alternatively, it can permit more aggressive downsizing, further shifting the engine operation into more efficient regions (Alger et al. (2008)). In particular, Zhong et al. (2013) reported that low pressure (LP) EGR (Fig. 1) is more suitable for the low RPM range whereas the high

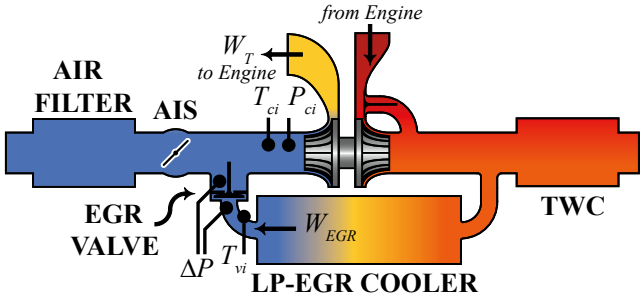

Fig. 1. LP-EGR configuration showing the flow rates and sensor measurements of interest.

⋆ Financial support was provided by the University of Michigan and Ford Alliance.

10.1016/j.ifacol.2016.08.105

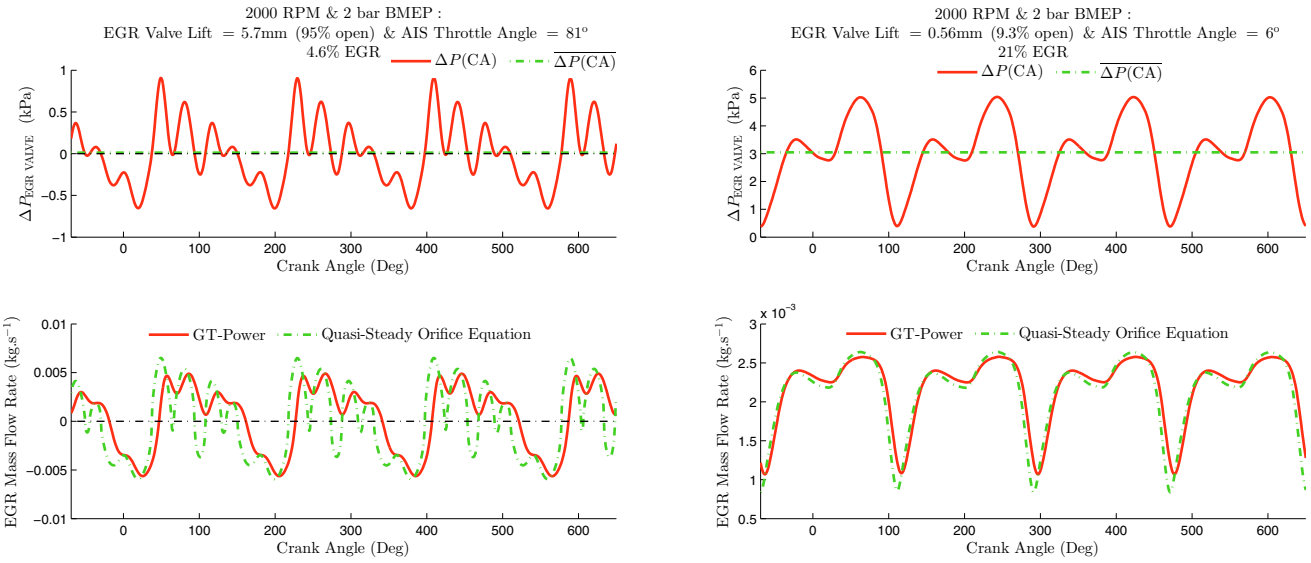

Fig. 2. Simulated pressure pulsations and EGR mass flow rate for 2 cases at 2000 RPM and 2 bar BMEP: 5.7 mm EGR valve lift and 81° (almost wide open) AIS throttle angle *(left)*, and 0.56 mm EGR valve lift and 6° AIS throttle angle *(right)*; estimated EGR mass flow rate using a quasi-steady orifice equation is shown as well.

pressure (HP) configuration is the better alternative at higher RPMs. However in either case, excessive amounts of EGR result in combustion instabilities (Heywood (1988)). The ability to accurately estimate and control the fraction of external EGR is therefore crucial to avoid the misfire and partial burn regions that can destroy any potential fuel economy gains with external EGR. Unfortunately, the typical small pressure differential (ΔP) and significant pressure pulsations across the LP-EGR valve challenge the estimation accuracy (Liu and Pfeiffer (2015)) and robustness of EGR control (Brewbaker (2015)). Introducing a pressure drop across the air intake system (AIS) throttle can considerably improve the LP-EGR percentage estimate (Liu and Pfeiffer (2015); Brewbaker (2015)). However, it is desirable to keep the average pressure differential ($\overline{\Delta P}$) at a minimum for better engine efficiency and transient response. Therefore, it is of interest to minimize AIS throttling (and consequently the ΔP across the EGR valve) without sacrificing EGR estimation accuracy.

This paper investigates the issue of estimating the mass flow rates of pulsating flows, in particular the difficulty of handling transient, reversing flows across a valve. The current work evaluates the application of different flow estimation methodologies to the estimation of EGR percentage with minimal AIS throttling using a ΔP measurement across the EGR valve in a LP-EGR configuration. Various ΔP measurement characteristics and flow formulations are considered. In Section 2, the challenge of estimating the pulsating flows encountered in LP-EGR systems using steady flow formulations is illustrated. In Section 3, the modeling of pulsating flow through a valve is first discussed, and the dependency of the error in estimated LP-EGR percentage on the ΔP measurement characteristics is covered in Section 4. Finally, concluding remarks are presented in Section 5.

2. PULSATIONS IN A LP-EGR LOOP

A 1-D gas dynamic simulation that solves continuity, 1-D momentum, and energy equations for compressible flows over a staggered grid was employed to investigate the LP-EGR flow in a turbocharged SI engine. In particular, using a 1-D GT-Power model for the Ford 1.6 L I4 EcoBoost engine with an added LP-EGR loop, the EGR valve lift and AIS throttle angle were swept for a range of engine speeds and break mean effective pressures (BMEP). BMEP values of 2, 5, 10, 15 and 20 bar, along with engine speeds of 1000, 1500, 2000 and 3000 RPM were chosen for this study, with maximum simulated BMEPs at 1000 and 1500 RPM of 10 and 15 bar respectively. The engine speed, AIS throttle angle and EGR valve lift are set as direct inputs. With the wastegate valve fully open, a throttler controller commands the engine throttle valve to achieve the desired BMEP. When the throttle valve saturates, a wastegate controller is activated to provide the necessary boost pressure to achieve the target BMEP.

Fig. 2 shows the simulated pressure pulsations and EGR mass flow rate for two sample cases. Both correspond to same engine RPM and load. The estimated EGR flow based on the crank-angle resolved ΔP signal using the steady compressible flow orifice equation is presented as well. Fig. 2 *(left)* shows a case with near wide open AIS throttle and EGR valve where the averaged differential pressure across the EGR valve ($\overline{\Delta P}$) was near zero ($\sim$ 0.01 kPa), with significant pulsations of $\sim$ 1.6 kPa, peak to trough. It can be seen that the mass flow rate reversal lags behind the sign reversal of the pressure differential due to the flow inertia, and in some cases, the sign reversal of ΔP is not followed by a mass flow reversal. However, this inertial effect is not captured by the steady compressible orifice equation, resulting in a –6.2% error

in the estimated percentage of EGR. Fig. 2 *(right)* shows a case with a higher $\overline{\Delta P}$ of $\sim$ 3 kPa where the ratio of the pressure pulsation peak-to-peak amplitude to $\overline{\Delta P}$ is significantly reduced. This was achieved by throttling the AIS and reducing the EGR valve lift [1] . A better agreement between the simulated and estimated EGR mass flow rate is observed in this case, which lacks flow reversal, and has an estimated EGR error of –0.35%.

3. MODELING OF A PULSATING FLOW THROUGH A VALVE

Severe pulsations about a zero mean pressure differential, as observed in Fig. 2 *(left)*, impose an inherent difficulty when estimating the EGR percentage with the steady compressible orifice equation. Therefore, an unsteady orifice equation that accounts for flow inertia is derived in this section. Previous work on modeling pulsating incompressible flows with an unsteady incompressible orifice equation, along with an analysis of pulsating flow estimation error sources are first reviewed. Afterward, an unsteady compressible flow orifice equation is derived, and an error analysis analogous to the incompressible case is presented.

3.1 Incompressible Fluid

McKee et al. and Gajan et al. investigated the sources of pulsating flow estimation errors present using the steady incompressible orifice equation $W \propto \sqrt{\Delta P}$ where W is the mass flow rate. Errors included the square root error (SRE) and the inertial error. The SRE is a result of the non-linearity of the square root function and accounts for the majority of the error when the averaged ΔP is used in the incompressible orifice equation. The averaging in the ΔP measurement can be due to a low frequency response ΔP transducer with built-in damping to attenuate fluctuation. Avoiding the SRE requires computing the mean of the square root of a rapidly sampled ΔP signal (McKee (1989); Gajan et al. (1992)). Consequently, the averaged flow is estimated with reasonable accuracy if the assumption of a quasi-steady flow holds. This is true when the Strouhal number $S_t = f d_e/\overline{U} << 1$ (f, d_e and $\overline{U}$ are the pulsation frequency, valve effective diameter and the bulk mean velocity respectively) (Gajan et al. (1992)). Otherwise, the inertia component, the first term within the 1-D momentum equation (Eq. (1)) should be accounted for:

$$\frac{\partial u}{\partial t} + u\frac{\partial u}{\partial x} + \frac{1}{\rho}\frac{\partial p}{\partial x} = 0 \tag{1}$$

where u, ρ and p are the velocity, density and pressure respectively. According to McKee (1989) and Gajan et al. (1992), integrating Eq. (1) with respect to x (from upstream to downstream of the valve) with the assumption of an incompressible fluid results in:

$$K_1\rho\frac{dW(t)}{dt} + K_2 W^2(t) = \rho\Delta P(t) \tag{2}$$

where K_2 is related to flow cross-sectional area and discharge coefficient. The term K_1 is independent of the pulsations (Gajan et al. (1992)), and $K_1 dW/dt$ accounts for the inertial effects. Other errors discussed by McKee et al. and Gajan et al. include flow coefficient shifts, gauge line amplification or attenuation, and pressure transducer response.

Depending on the value of ΔP, the assumption of an incompressible fluid (ρ = constant) can be inappropriate for the flow across the EGR valve. In this paper, an equation analogous to Eq. (2) is derived for a compressible flow and is presented in the subsequent subsection. Errors resulting from the different formulations – analogous to those of the incompressible fluid case – are then discussed.

3.2 Compressible Flow

It is a common practice in engine modeling to estimate flow through valves (e.g. throttle and poppet valves) with the steady compressible isentropic flow orifice equation. The effect of non-ideal behaviors resulting from irreversibility, is accounted for by introducing the discharge coefficient, C_D (Guzzella and Onder (2009)). Using the same logic, an isentropic process with ratio of specific heats γ: $\rho = \rho_0\left(\frac{p}{p_0}\right)^{\frac{1}{\gamma}}$ can be assumed for a flow from upstream of the valve (x_0) to the valve throat (x_T) where $x_0 < x_T$ and the flow is in the positive x-direction. The 1-D momentum equation for compressible and inviscid flow expressed in the non-conservative form (Eq. (1)) is rewritten as:

$$\frac{\partial u}{\partial t} + u\frac{\partial u}{\partial x} + \frac{p_0^{\frac{1}{\gamma}}}{\rho_0}\frac{1}{p^{\frac{1}{\gamma}}}\frac{\partial p}{\partial x} = 0. \tag{3}$$

Integrating from x_0 to x_T with pressures p_0 and p_T at x_0 and x_T respectively, and assuming that $u_0 \simeq 0$, we get

$$\int_{x_0}^{x_T}\frac{\partial u}{\partial t}dx + \frac{u_T^2}{2} + \frac{p_0^{\frac{1}{\gamma}}}{\rho_0}\int_{p_0}^{p_T} p^{-\frac{1}{\gamma}}dp = 0. \tag{4}$$

Realizing that:

$$u = \frac{W}{\rho A} = \frac{W}{\rho_0 A}\frac{p_0^{\frac{1}{\gamma}}}{p^{\frac{1}{\gamma}}}$$

where A is the cross-sectional area at x, Eq. (4) can be rewritten as:

$$\frac{p_0^{\frac{1}{\gamma}}}{\rho_0}\int_{x_0}^{x_T}\frac{1}{A}\frac{\partial}{\partial t}\left(\frac{W}{p^{\frac{1}{\gamma}}}\right)dx + \frac{W_T^2}{2A_T^2\rho_0^2}\left(\frac{p_0}{p_T}\right)^{\frac{2}{\gamma}} = \frac{p_0^{\frac{1}{\gamma}}}{\rho_0}\frac{\gamma}{\gamma-1}\left(p_0^{\frac{\gamma-1}{\gamma}} - p_T^{\frac{\gamma-1}{\gamma}}\right) \tag{5}$$

where A_T represents the valve cross-sectional area at the valve throat. The variation of W and p in x can be assumed to be minor from x_0 up to a small distance just before the valve throat x_T. Neglecting the contribution of this dependency on x near the throat on the integral term in Eq. (5), the following simplifications can be used: $W_T \simeq W(x) \simeq W$ and $p(x) \simeq p_0$. Substituting for p_T/p_0 and ρ_0 by P_r and $p_0/(RT_0)$ respectively, where R and T_0 denote the flow's ideal gas constant and upstream temperature, introducing C_D to account for non-ideal behaviors of the flow, and rearranging Eq. (5), we obtain:

[1] In the regions of interest where EGR improves engine efficiency, the reduced EGR valve lift contributes to the increased $\overline{\Delta P}$ while BMEP is maintained. Larger pressure drops in the pre-compressor and post-turbine piping accompany the higher air mass flow rate required to maintain the same load as efficiency drops with the reduced EGR percentage. The lower compressor inlet and higher turbine outlet pressures result in a higher $\overline{\Delta P}$ across the EGR valve.

$$2C_D^2 A_T^2 P_r^{\frac{2}{\gamma}} \frac{p_0^{\frac{\gamma+1}{\gamma}}}{RT_0} \frac{d}{dt}\left(\frac{W}{p_0^{\frac{1}{\gamma}}}\right) \int_{x_0}^{x_T} \frac{dx}{A} + W^2 = \Psi^2\left(P_r, p_0, T_0\right) \tag{6}$$

where:

$$\Psi\left(P_r, p_0, T_0\right) = C_D A_T \frac{p_0}{\sqrt{RT_0}} P_r^{\frac{1}{\gamma}} \sqrt{\frac{2\gamma}{\gamma-1}\left(1 - P_r^{\frac{\gamma-1}{\gamma}}\right)} \tag{7}$$

is the steady compressible isentropic flow orifice equation (for the $P_r \geq P_{r,CR} \equiv$ the critical pressure ratio). Further assuming that the variation of p_0 with t far less significant than that of W with t (the fluctuations in p_0 with respect to its average value are small compared to those of ΔP); hence, $d\left(W p_0^{-\frac{1}{\gamma}}\right)/dt \simeq p_0^{-\frac{1}{\gamma}} dW/dt$, Eq. (6) can be rewritten as:

$$\widetilde{K}_1 C_D^2 A_T^2 \Phi\left(P_r, p_0, T_0\right) \frac{dW}{dt} + W^2 = \Psi^2\left(P_r, p_0, T_0\right) \tag{8}$$

where $\widetilde{K}_1$ is a function of the valve geometry and lift, and

$$\Phi\left(P_r, p_0, T_0\right) = \frac{p_0}{RT_0} P_r^{\frac{2}{\gamma}}. \tag{9}$$

Without the assumption that $d\left(W p_0^{-\frac{1}{\gamma}}\right)/dt \simeq p_0^{-\frac{1}{\gamma}} dW/dt$, we obtain:

$$\begin{aligned} \widetilde{K}_1 C_D^2 A_T^2 \Phi\left(P_r, p_0, T_0\right)\left(\frac{dW}{dt} - W\frac{\ln p_0}{\gamma}\right) + W^2 \\ = \Psi^2\left(P_r, p_0, T_0\right). \end{aligned} \tag{8*}$$

Including the additional term in Eq. (8*) had a negligible effect on the flow estimates discussed in Section 4; the assumption used to obtain Eq. (8) is therefore valid under the conditions studied.

The above derivation was performed for forward flow where $x_0 < x_T$. When the flow reverses direction, the upstream pressure p_0 and temperature T_0 then refer to the pressure and temperature at some $x_0 > x_T$, and the integration of Eq. (3) should be carried out from x_T to x_0 resulting in the replacement of W^2 and Ψ^2 in Eq. (8) by $-W^2$ and $-\Psi^2$ respectively. In addition, C_D and $\widetilde{K}_1$ can assume different values depending on the flow direction. The equivalent of Eq. (8) that accounts for the flow reversal is detailed in the subsequent section.

Dropping the transient term dW/dt, Eq. (8) reduces to the steady compressible flow orifice equation (Eq. (7)). As was the case for an incompressible fluid, two mass flow rate formulations that exclude the inertial term – based on either cycle-averaged or instantaneous (fast-sampled) measurements – are considered. If only an averaged $\overline{\Delta P}$ and p_0 measurements were available, denoted by $\overline{\Delta P}$ and $\overline{p_0}$ respectively, P_r is then computed as $P_r = 1 - \overline{\Delta P}/\overline{p_0}$. In this case, feeding this P_r into Eq. (7): $\overline{W} = \Psi\left(1 - \overline{\Delta P}/\overline{p_0}, \overline{p_0}, \overline{T_0}\right)$, results in a non-linearity error – similar to the SRE – which is expected to contribute to the majority of flow estimation error. This error is eliminated with the use of a sufficiently fast sampled ΔP signal, and the flow estimate is sufficiently accurate if the quasi-steady assumption holds. If inertial effects are significant, then the use of Eq. (8) would be justified. The parameter $\widetilde{K}_1$ in Eq. (8) is assumed to be independent of the pulsations, similar to K_1 in Eq. (2). However, the effect of pulsations on the inertial term is accounted for to some extent by Φ.

4. ERROR IN ESTIMATED LP-EGR PERCENTAGE

4.1 Comparison of Compressible EGR Flow Formulations

The 1-D GT-Power SI-engine model (described in Section 2) is now employed to investigate the impact of using the averaged, quasi-steady and unsteady compressible flow formulations on the error in the EGR percentage over a range of engine speeds and loads. The temperature at the EGR valve inlet temperature T_{vi} (Fig. 1) along with the pressure and temperature upstream of the compressor (p_{ci} and T_{ci} respectively) are time averaged over the engine cycle. The gauge line lengths for the ΔP measurement are assumed to be zero. The ΔP measurement is either cycle averaged or crank-angle (CA) resolved in this subsection depending upon the orifice equation formulation used. The quasi-steady and unsteady formulations require all pressure and temperature signals to be sampled at a sufficient rate. However, sampling all four signals at every CA degree results in minor improvement compared to the case where only the ΔP signal is CA-resolved.

The pressure p_{vo} at the ΔP sensor tap downstream the EGR valve is different from p_T in the derivation presented in the preceding section. It is expected that p_{vo} is somewhat larger than p_T due to pressure recovery taking place downstream the valve throat. However, the effect of pressure recovery is lumped, along with other deviations from the ideal case, in the discharge coefficient which is a function of both valve lift and ΔP. Finally, it is justified to assume that $p_{vo} \simeq p_{ci}$ as there is no flow restriction between the EGR valve outlet and the compressor inlet.

To account for choking and flow reversal (the direction of the flow is not apparent in the terms W^2 and Ψ^2), Eq. (8) is rewritten as:

$$\begin{aligned} \widetilde{K}_1 C_D^2 A_T^2 \widetilde{\Phi}\left(\Delta P, p_{ci}, T_{vi}, T_{ci}\right) dW/dt + W|W| \\ = \widetilde{\Psi}|\widetilde{\Psi}|\left(\Delta P, p_{ci}, T_{vi}, T_{ci}\right) \end{aligned} \tag{10}$$

where the functions $\widetilde{\Psi}$ and $\widetilde{\Phi}$ are defined as

$$\widetilde{\Psi}\left(\Delta P, p_{ci}, T_{vi}, T_{ci}\right) = \begin{cases} \Psi\left(P_r, p_{ci} + \Delta P, T_{vi}\right) & \text{if } \Delta P \geq 0 \\ -\Psi\left(P_r, p_{ci}, T_{ci}\right) & \text{if } \Delta P < 0 \end{cases} \tag{11}$$

and

$$\widetilde{\Phi}\left(\Delta P, p_{ci}, T_{vi}, T_{ci}\right) = \begin{cases} \Phi\left(P_r, p_{ci} + \Delta P, T_{vi}\right) & \text{if } \Delta P \geq 0 \\ \Phi\left(P_r, p_{ci}, T_{ci}\right) & \text{if } \Delta P < 0 \end{cases}, \tag{12}$$

and finally, the pressure ratio P_r is computed as

$$P_r = \begin{cases} \max\left(p_{ci}/\left(p_{ci} + \Delta P\right), P_{r,CR}\right) & \text{if } \Delta P \geq 0 \\ \max\left(1 + \Delta P/p_{ci}, P_{r,CR}\right) & \text{if } \Delta P < 0 \end{cases}. \tag{13}$$

Denoting the estimated EGR flow rate by $\widehat{W}_{EGR}$ and the GT-Power predicted EGR and total mass flow rate by W_{EGR} and W_{TOTAL} respectively, the error in the estimated EGR percentage ϵ is defined as:

$$\epsilon = 100\frac{\widehat{W}_{EGR} - W_{EGR}}{W_{TOTAL}}. \tag{14}$$

The estimated EGR flow $\widehat{W}_{EGR}$ is computed based on 3 different formulations: (*1*) steady orifice equation with

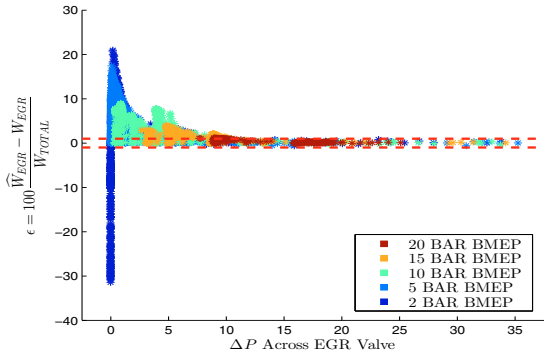

(a)

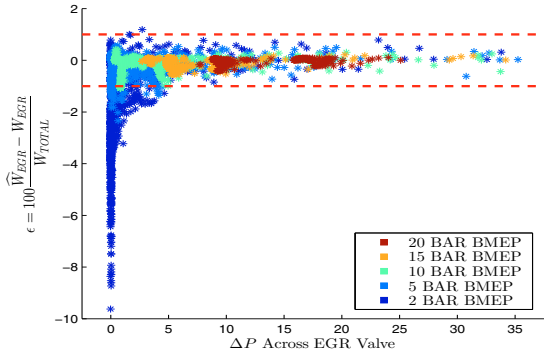

(b)

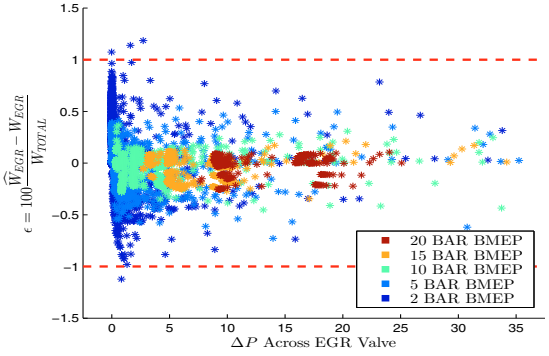

(c)

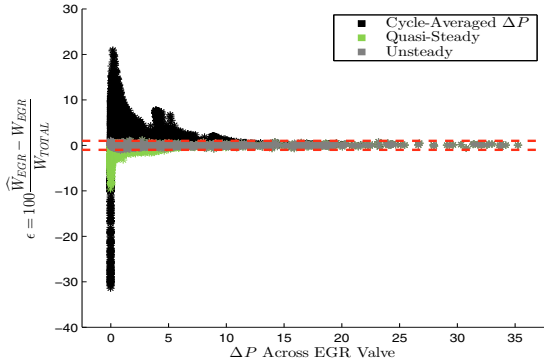

(d)

Fig. 3. Error in the estimate of EGR percentage versus ΔP using cycle-averaged ΔP (a), quasi-steady orifice equation with CA resolved ΔP (b), unsteady orifice equation and CA resolved ΔP (c). All 3 cases *(a)*, *(b)* and *(c)* are shown in *(d)*. The $\pm 1\%$ error bounds are shown in all subplots with dashed red lines.

cycle-averaged ΔP, *(2)* steady orifice equation with CA-resolved ΔP (quasi-steady), and *(3)* unsteady orifice equation with CA-resolved ΔP (Eq. (10)). The steady orifice equation in formulations *(1)* and *(2)* is equivalent to Eq. (10) with $\widetilde{K}_1 = 0$. The data for W_{EGR}, W_{TOTAL}, ΔP, p_{ci}, T_{ci} and T_{vi} is obtained using the 1-D GT-Power model discussed in Section 2 for engine speeds and BMEP's of 1000, 1500, 2000 and 3000 RPM and 2, 10, 15 and 20 bar respectively. For each speed-load combination, the AIS throttle angle and EGR valve lift are swept from near fully closed to near wide open. Cases with AIS throttle angle and EGR valve lift values requiring turbocharger speeds in excess of allowable limits, or where the wastegate controller saturates and fails to reach the target BMEP, are discarded.

Fig. 3 depicts the error ϵ obtained using these formulations plotted versus the cycle-averaged ΔP for all simulated engine operating points; the ± 1 % error bounds are shown as well. For the unsteady formulation (Fig. 3 *(c)*), the $\widetilde{K}_1 C_D^2 A_T^2$ values that minimize the sum of squares of the difference between the right and left hand sides of Eq. (10) for cases where $S_t > 0.1$ were first computed using CA resolved W_{EGR} predicted by GT-Power, then fit as a function of the EGR valve lift using a 3$^{\text{rd}}$ order polynomial (Fig. 4). The resulting fit for $\widetilde{K}_1 C_D^2 A_T^2$ is then used to generate the data shown in Fig. 3 *(c)*. Figure 5 shows the EGR mass flow rates versus crank angle for the first case presented in Fig. 2 with the additional curve for estimated EGR flow using Eq. (10). The estimated flow using the unsteady orifice equation with inertial term strongly agrees with the simulated flow using GT-Power.

The non-linearity error is, as expected, the major contributor to ϵ as can observed from the significant improvement achieved when CA resolved ΔP values (quasi-steady) are used instead of their cycle-averaged counterparts; the minimum $\overline{\Delta P}$ required to keep ϵ within the ± 1 % bound is reduced from around 10 to 4 kPa (Fig. 3 *(a)* and *(b)*). The contribution of the inertial effects to ϵ becomes significant for $\overline{\Delta P}$ values smaller than 4 kPa, especially for low load and high RPM cases (Fig. 6). At lower engine loads and RPMs, W_{TOTAL} is smaller hence the error in $\widehat{W}_{EGR}$ propagated to ϵ becomes more apparent. In addition, the larger pulsation frequency f at higher engine speeds requires higher EGR flow velocities $\overline{U}$ and consequently higher $\overline{\Delta P}$ to keep S_t low and the quasi-steady assumption valid. It should be noted here that even if the sole interest behind using LP-EGR was knock suppression at high loads, it is still valuable to accurately estimate the LP-EGR percentage with minimal AIS throttling at lower loads since LP-EGR can be employed during transient engine operation. Finally, accounting for the inertia term using Eq. (10) results in ϵ within ± 1 % for all $\overline{\Delta P}$ except for 4 simulated points (less than 0.1 % of the total number of simulated cases where ϵ does not exceed ± 1.2 %).

4.2 Sampling Rate & ΔP Sensor Response

In this section, the effect of the ΔP sensor response and output signal sampling frequency f_S is investigated to establish a middle ground solution with some intermediate f_S that can achieve the desired estimation accuracy while

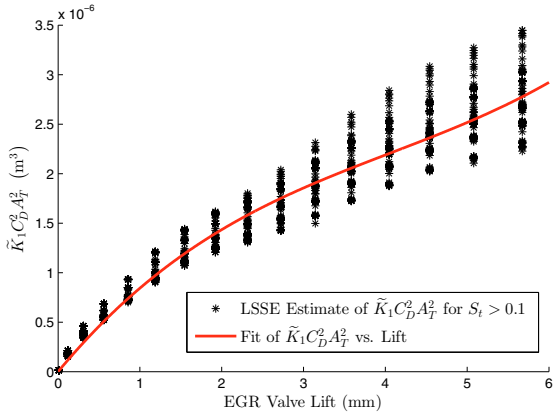

Fig. 4. Least sum of square error (LSSE) estimates of $\widetilde{K}_1 C_D^2 A_T^2$ versus EGR valve lift for $S_t > 0.1$.

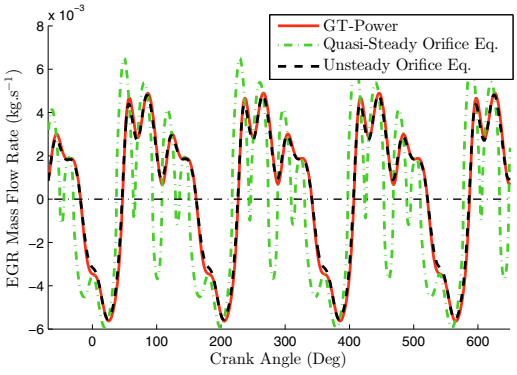

Fig. 5. Simulated and estimated EGR mass flow rates for 2000 RPM, 2 bar BMEP, 5.7 mm EGR vavle lift and and 81^o (almost wide open) AIS throttle angle.

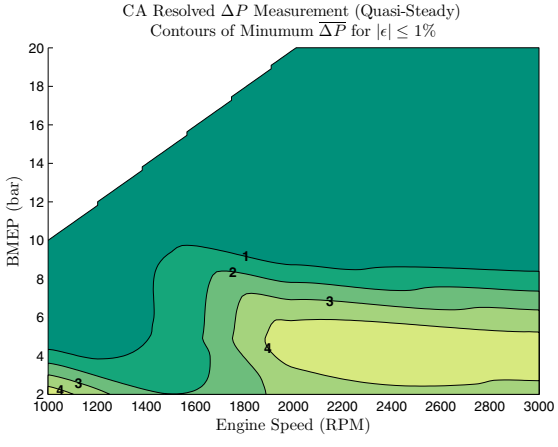

Fig. 6. Contours of the minimum $\overline{\Delta P}$ for $\epsilon \leq \pm 1$ % over the simulated engine operating conditions when the quasi-steady formulation is used.

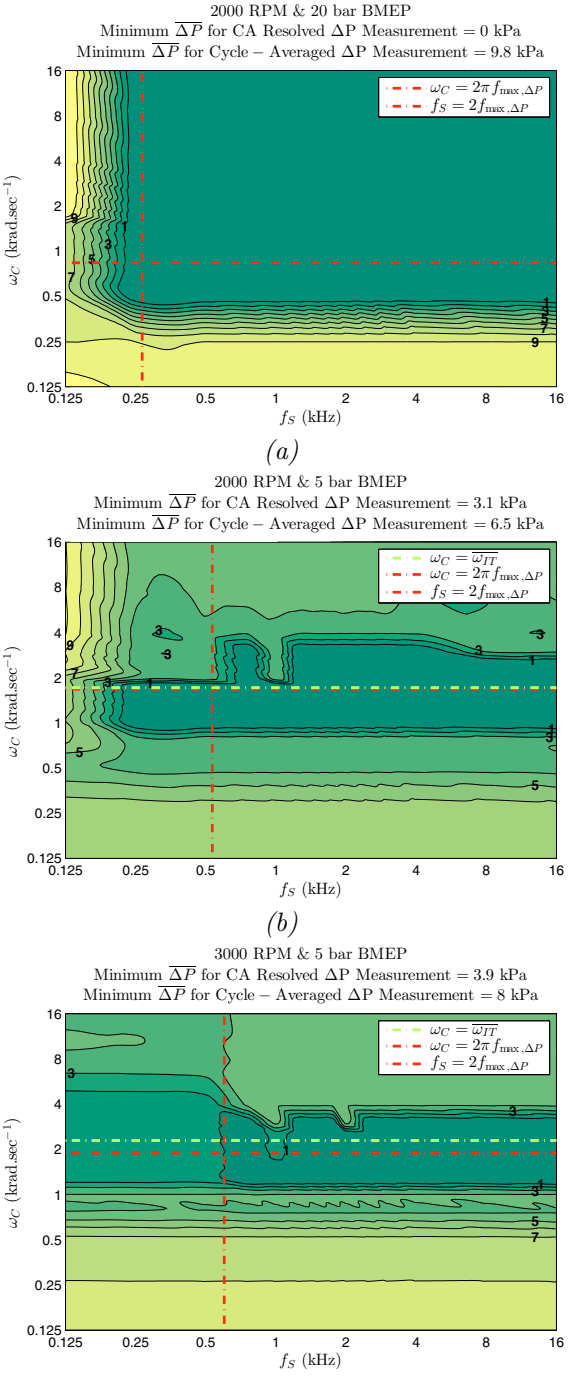

Fig. 7. Contours of $\min_{|\epsilon| \leq 1\%} \left(\overline{\Delta P}\right)$ versus f_S and ω_C for *(a)* 2000 RPM and 20 bar BMEP, *(b)* 2000 RPM and 5 bar BMEP and *(c)* 3000 RPM and 5 bar BMEP.

still being practically and economically feasible. For each of the simulated engine operating points, the sampling frequency is swept from 125 Hz to 16 kHz (sampling at every degree CA corresponds to 6 kHz and 18 kHz at 1000 and 3000 RPM respectively). The ΔP sensor response is assumed to be that of a 1$^{\text{st}}$ order lag with cut-off frequency ω_C, and is modeled for by filtering the CA resolved ΔP predicted by GT-Power. Values of ω_C ranging between 125 rad.s^{-1} and 16 krad.s^{-1} are considered.

Figure 7 *(a)* shows the contours of the minimum $\overline{\Delta P}$ required for maintaining ϵ within ± 1 % at 2000 RPM and 20 bar BMEP versus f_S and ω_C when the quasi-steady compressible flow formulation is used. As ω_C and f_S are increased beyond $\omega_{max,\Delta P} = 2\pi f_{max,\Delta P}$ and $2 f_{max,\Delta P}$ respectively where $f_{max,\Delta P}$ denotes the highest frequency

present [2] in ΔP, $\min_{|\epsilon|\leq 1\%}\left(\overline{\Delta P}\right)$ converges to that of the corresponding quasi-steady case sampled at every CA degree. A different behavior, however, is observed for the low load cases (Fig. 7 *(b)* and *(c)*) where the inertial effects are considerable. The minimum error $\min_{|\epsilon|\leq 1\%}\left(\overline{\Delta P}\right)$ decreases as f_S is increased with ω_C fixed; however its variation is not monotonic with ω_C for some values of f_S. Islands of f_S and ω_C also exist where the restriction $\min_{|\epsilon|\leq 1\%}\left(\overline{\Delta P}\right)$ (less the 0.5 kPa) is looser compared to the corresponding quasi-steady case (3.1 and 3.9 kPa at 5 bar BMEP and 2000 and 3000 RPM respectively). The lag introduced by the ΔP sensor response is mimicking the effect of the inertial term, which improves the EGR percentage estimate of the quasi-steady orifice equation.

For simplicity, the case for an incompressible fluid is revisited here. Assuming that the inertia term can be modeled with a 1st order lag in ΔP [3] with a time constant of $1/\omega_{IT}$, such that:

$$\Delta P - \Delta P_{IT} = \frac{1}{\omega_{IT}}\frac{d\Delta P_{IT}}{dt} \tag{15}$$

and

$$W = \Psi^*\left(\Delta P_{IT}\right) = \text{sign}\left(\Delta P_{IT}\right)\sqrt{\frac{\rho|\Delta P_{IT}|}{K_2}} \tag{16}$$

$$\Rightarrow \frac{dW}{dt} = \frac{1}{2}\sqrt{\frac{\rho}{|\Delta P_{IT}|K_2}}\frac{d\Delta P_{IT}}{dt}. \tag{17}$$

Accounting for flow reversal, Eq. (2) can be rewritten as:

$$\rho\frac{K_1}{K_2}\frac{dW}{dt} + W|W| = \Psi^*|\Psi^*|\left(\Delta P\right). \tag{18}$$

Combining equations (15) through (18):

$$\rho\frac{K_1}{K_2} = \frac{2}{\omega_{IT}}|W|, \tag{19}$$

and substituting Eq. (19) into (18), we obtain:

$$\frac{2}{\omega_{IT}}|W|\frac{dW}{dt} + W|W| = \Psi^*|\Psi^*|\left(\Delta P\right). \tag{20}$$

Assuming that the incompressible case has an analogous form of Eq. (20), we end up with

$$\frac{2}{\omega_{IT}}|W|\frac{dW}{dt} + W|W| = \widetilde{\Psi}|\widetilde{\Psi}|\left(\Delta P, p_o, T_i, T_o\right). \tag{21}$$

The ω_{IT} values minimizing the sum of squares of the difference between the right and left hand side of Eq. (21) are computed for the cases with $St > 0.1$, where the pulsation frequency f is set to the highest frequency of the significant frequency components of ΔP. Contour lines for ω_C equal to the mean of the computed ω_{IT} for the cases at 5 bar BMEP and 2000 and 3000 RPM are shown on Fig. 7 *(b)* and *(c)*. The islands with lowest $\min_{|\epsilon|\leq 1\%}\left(\overline{\Delta P}\right)$ are in the vicinity of the line $\omega_C = \overline{\omega_{IT}}$. The lag introduced in ΔP indeed emulates the addition of the inertial term and hence can improve the estimates of the quasi-steady formulation. Figure 8 shows the error ϵ versus $\overline{\Delta P}$ for $f_S = 1$ kHz and $\omega_C = 1$, 1.5 and 2 krad.s^{-1} compared to the quasi-steady and unsteady orifice equations fed by the CA resolved ΔP. The error ϵ for a cut-off frequency

[2] Highest frequency whose corresponding amplitude is significant.

[3] Analogously, a lag in the pressure ratio can be introduced to account for transient effects in compressors as can be seen the work of Grietzer on modeling compressor surge (Greitzer (1976)).

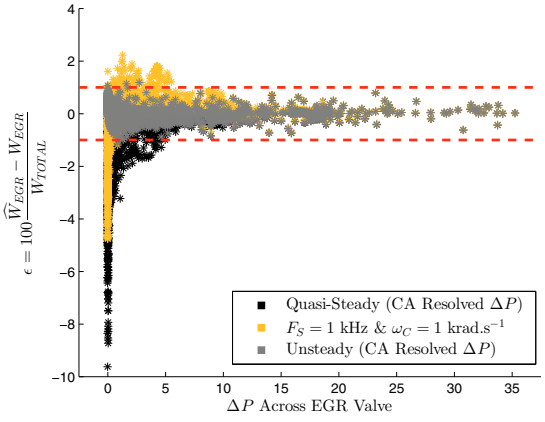

(a)

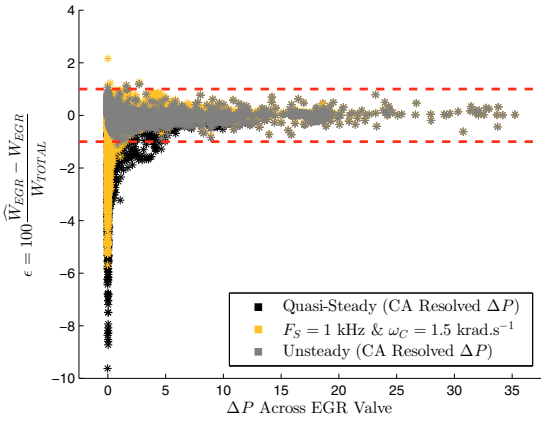

(b)

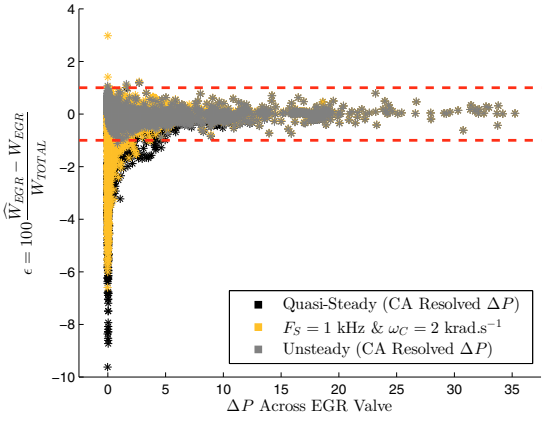

(c)

Fig. 8. Error in the estimate of EGR percentage versus ΔP using cycle-averaged ΔP for $f_S = 1$ kHz and *(a)* $\omega_C = 1$ krad.s^{-1}, *(b)* $\omega_C = 1.5$ krad.s^{-1} and *(c)* $\omega_C = 2$ krad.s^{-1} compared to the quasi-steady and unsteady formulations fed by CA resolved ΔP.

ω_C of 1.5 krad.s^{-1} is, in general, reduced relative to that where ω_C's 1 and 2 krad.s^{-1}. However, regions exist where ω_C's of 1 or 2 krad.s^{-1} produce better results due to the dependency of ω_{IT} on EGR flow.

The unsteady orifice equation using a CA-resolved ΔP measurement with negligible sensor lag provides sufficient EGR flow estimation accuracy without restricting the range of allowable $\overline{\Delta P}$. However, this approach is com-

putationally expensive for real time estimation, especially when EGR valve lifts and the term $\widetilde{K}_1 C_D^2 A_T^2$ are small, which requires small time steps to simulate the dynamic system in Eq. (10). Such an approach would be problematic and expensive to implement in an EGR controller. On the other hand, using cycle-averaged ΔP for real time EGR flow estimation is straightforward but considerably restricts the allowable range of $\overline{\Delta P}$ to larger values, leading to diminished engine efficiency improvements. The quasi-steady formulation with a sampling frequency of 1 kHz and a ΔP sensor time constant of 0.67 ms ($\omega_C = 1.5$ krad.s^{-1}) provides a middle ground solution. This approach is on average ~ 14 times less computationally expensive than the unsteady formulation with CA-resolved ΔP, and is more feasible for controller implementation while enabling a wide range of $\overline{\Delta P}$.

5. SUMMARY AND CONCLUSIONS

The current work investigated two compressible orifice equation formulations, one the classical steady state approximation and the other a newly developed transient equation. The latter was critical for the accurate modeling of pulsating flows with low pressure drops across the orifice. Various ΔP transducer responses and output sampling frequencies were also investigated.

Significant pressure pulsations across the EGR valve typical of LP-EGR configurations result in % EGR estimation errors in estimated EGR percentage (ϵ) that can be as high as 30% when the steady compressible orifice equation is used with a cycled-averaged ΔP measurement. With this approach, the average ΔP should be kept above 10 kPa for ϵ to fall within $\pm 1\%$. Neglecting the effect of gauge line amplification and attenuation, and with the availability of a fast response ΔP sensor capable of accurately measuring ΔP at every CA degree, the use of the steady orifice equation can reduce $\min_{|\epsilon| \leq 1\%} \left(\overline{\Delta P}\right)$ to 4 kPa. Further improvements are possible by accounting for flow inertia with the unsteady compressible orifice equation derived in this paper, where ϵ remains bounded within $\pm 1\%$ even as $\overline{\Delta P}$ approaches zero.

When using the steady orifice equation in conjunction with a ΔP transducer with a non-negligible lag, the dependency of ϵ on the sensor's response is non-monotonic. If the sensor's time constant falls within an interval that mimics the inertial effects of the flow, then the EGR percentage estimate can instead be improved relative to a faster sensor. A minimum ΔP of 1 kPa that guarantees an ϵ within $\pm 1\%$ is possible with a sensor time constant of 0.67 ms and a sampling frequency of 1 kHz.

REFERENCES

Alger, T., Chauvet, T., and Dimitrova, Z. (2008). Synergies between high EGR operation and GDI systems. In *SAE Technical Paper*, 2008-01-0134.

Brewbaker, T. (2015). Multivariable diesel low-pressure EGR controller designed by input-output linearization. In *American Control Conference (ACC), 2015*, 31–37. doi:10.1109/ACC.2015.7170707.

Gajan, P., Mottram, R., Hebrard, P., Andriamihafy, H., and Platet, B. (1992). The influence of pulsating flows on orifice plate flowmeters. *Flow Measurement and instrumentation*, 3(3), 118–129.

Greitzer, E.M. (1976). Surge and rotating stall in axial flow compressors Part I: Theoretical compression system model. *Journal of Engineering for Gas Turbines and Power*, 98(2), 190–198.

Guzzella, L. and Onder, C. (2009). *Introduction to modeling and control of internal combustion engine systems*. Springer Science & Business Media Berlin.

Heywood, J.B. (1988). *Internal combustion engine fundamentals*. Mcgraw-Hill New York.

Hoepke, B., Jannsen, S., Kasseris, E., and Cheng, W.K. (2012). EGR effects on boosted SI engine operation and knock integral correlation. In *SAE Technical Paper*, 2012-01-0707.

Liu, F. and Pfeiffer, J. (2015). Estimation algorithms for low pressure cooled egr in spark-ignition engines. *SAE International Journal of Engines*, 8(2015-01-1620).

McKee, R. (1989). Pulsation effects on orifice metering considering primary and secondary elements. *Proc. of the 22nd Gulf Coast Measurements Short Course*, 112–118.

Potteau, S., Lutz, P., Leroux, S., Moroz, S., and Tomas, E. (2007). Cooled EGR for a turbo SI engine to reduce knocking and fuel consumption. In *SAE Technical Paper*, 2007-01-3978.

Teodosio, L., De Bellis, V., and Bozza, F. (2015). Fuel economy improvement and knock tendency reduction of a downsized turbocharged engine at full load operations through a low-pressure EGR system. In *SAE Technical Paper*, 2015-01-1244.

Westin, F., Grandin, B., and Ångström, H.E. (2000). The influence of residual gases on knock in turbocharged SI-engines. In *SAE Technical Paper*, 2000-01-2840.

Zhong, L., Musial, M., Reese, R., and Black, G. (2013). EGR systems evaluation in turbocharged engines. In *SAE Technical Paper*, 2013-01-0936.